INSTITUTE OF FLUID-FLOW MACHINERY
POLISH ACADEMY OF SCIENCES

# TRANSACTIONS OF THE INSTITUTE OF FLUID-FLOW MACHINERY

## 108

GDAŃSK 2001

## TRANSACTIONS OF THE INSTITUTE OF FLUID-FLOW MACHINERY

Appears since 1960

**Aims and Scope**

*Transactions of the Institute of Fluid-Flow Machinery* have primarily been established to publish papers from four disciplines represented at the Institute of Fluid-Flow Machinery of Polish Academy of Sciences, such as:

- Liquid flows in hydraulic machinery including exploitation problems,
- Gas and liquid flows with heat transport, particularly two-phase flows,
- Various aspects of development of plasma and laser engineering,
- Solid mechanics, machine mechanics including exploitation problems.

The periodical, where originally were published papers describing the research conducted at the Institute, has now appeared to be the place for publication of works by authors both from Poland and abroad. A traditional scope of topics has been preserved.

Only original and written in English works are published, which represent both theoretical and applied sciences. All papers are reviewed by two independent referees.

## EDITORIAL AND PUBLISHING OFFICE

IFFM Publishers (Wydawnictwo IMP), Institute of Fluid Flow Machinery, Fiszera 14, 80-952 Gdańsk, Poland, Tel.: +48(58)3411271 ext. 141, Fax: +48(58)3416144, E-mail: esli@imp.gda.pl



Financial support of publication of this journal is provided by the State Committee for Scientific Research, Warsaw, Poland

### Terms of subscription

Subscription order and payment should be directly sent to the Publishing Office

### Warunki prenumeraty w Polsce

Wydawnictwo ukazuje się przeciętnie dwa lub trzy razy w roku. Cena numeru wynosi 20,- zł + 5,- zł koszty wysyłki. Zamówienia z określeniem okresu prenumeraty, nazwiskiem i adresem odbiorcy należy kierować bezpośrednio do Wydawcy (Wydawnictwo IMP, Instytut Maszyn Przepływowych PAN, ul. Gen. Fiszera 14, 80-952 Gdańsk). Osiągalne są również wydania poprzednie. Prenumerata jest również realizowana przez jednostki kolportażowe RUCH S.A. właściwe dla miejsca zamieszkania lub siedziby prenumeratora. W takim przypadku dostawa następuje w uzgodniony sposób.

**ISSN 0079-3205**

TRANSACTIONS OF THE INSTITUTE OF FLUID-FLOW MACHINERY

No. 108, 2001, 33-45

TEODOR BRECZKO[1], KRZYSZTOF KUS[1]

# Residual stresses and shape memory effect

It is possible to estimate the reliability of the materials during their use by recording the changes in defect density of polycrystalline structure, which can be estimated on residual stresses at a crystal micro-level. In this paper the experimental results of the residual stress field changes in actuator manufactured using shape memory alloy (SMA) are presented. The experimental data are based on the investigation of the changes in the root-mean-square (RMS) micro-strains and size of coherent block in the SMA caused by thermal and mechanical loading. The study is performed on the samples of approximately equiatomic TiNi alloy. To induce the reversible martensite transformations in the material the external loading is applied with subsequent data recording using the X-ray method. The results of experimental measurements of the RMS microst rain and coherent block size in austenite are presented. Basing on the experimental data a modified (by Brechko [4-5]) mathematical model of Likhachev and Malinin [3] is proposed, which is used in the computer simulations including the martensite transformations, twining, elastic and irreversible deformations. The experimental and computer modeling results of stress and strain field generated by the defects in polycrystalline materials are discussed.

## 1. Introduction

Degradation of functional properties and fatigue of SMAs has been formulated by R. Stalmans and J. Van Humbeck [1] as follows: "... the reliability of shape memory devices depends on its global lifetime performance. The failure of SMA-elements is completely different from the failure of conventional materials; SMAs can fail due to a decrease of the stroke during repeated actuation, due to a shift of the transformation temperatures, etc. Moreover, degradation and fatigue are influenced in a complex way by many parameters. Time, maximum temperature, maximum stress, maximum strain, strain mode and the amount of cycles are in this respect important external parameters. Important internal parameters that can have a strong influence on the lifetime are: the alloy system, the alloy composition, the heat treatment, and the processing. For general purposes, the maximum memory effect, strain and/or stress, will be selected depending on the

[1]University of Warmia and Mazury, Faculty of Engineering Sciences, ul. Oczapowskiego 11, 10-957 Olsztyn, Poland

required amount of cycles".

Application of SMAs in various areas of engineering [2] are by all means connected to time of preservation of their functional properties. They find also various applications in engineering as bent elements. In these condition changes of stresses at a bend complicates martensite transformation on section. Therefore in the present work carried out researches in conditions are approached to such conditions work of a material. The basic purpose of these researches is to search for structural parameters on which it will be possible to predict a temporary resource of non-failure operation of elements from shape memory alloys.

Let us to consider the SMA based on the Ti and Ni. Despite it can be plastically deformed at some relatively low temperature, upon exposure to certain higher temperature SMA returns to its original shape prior to the deformation since the molecular bonds are not broken. If overloading occurs, then lattice will break the bonds and shape will not be fully recovered. Materials that exhibit shape memory only upon heating are referred to as having a one-way shape memory. Some materials also undergo a change in shape upon recooling. These materials are said to have a two-way shape memory. In order to understand the way, in which the shape memory effect works, it is useful to examine the crystal structure of SMA. All shape memory alloys exhibit two significantly distinct crystal structures or phases. The presence of the particular phase depends on the temperature and amount of stress (think of it as an internal stresses) being applied to the SMA. These phases are known as martensite, which exist at lower temperatures, and austenite for higher temperatures.

## 2. Experiment

For the experiment an $Ni_{50.6}$ $Ti_{49.4}$ SMA has been used. The samples of SMA with the size 70 x 2 mm were cut from a 3 mm thick sheet. After this, the sample was annealed at temperature of 825 K for one hour. After annealing, the sample has been subjected to a cyclic thermo-mechanical loading. For this research the special stand has been used (Fig. 1). The tripod (2) was attached to the base (1). On the end of tripod a sample SMA was placed. One end of the sample is fixed (3) and the other one is loaded (4). For heating purposes the electrical system (6) has been coupled to the sample. In the experiment the one-way shape memory effect has been generated, according to the scheme presented in Fig. 2. The characteristic temperatures of alloy are: $A_s = 300$ K, $A_f = 308$ K, $M_s = 291$ K and $M_f = 283$ K.

In our case, the cyclic thermal and mechanical loading proceeded in the following manner: first, we cool the sample down to the temperature of 250 K , after that, the sample is bent at angle velocity approximately equal to $30^o$ per second and heated to 350 K (Fig. 3). In the experimental study the total applied strain level for the NiTi specimens was estimated at 6 %. During the cooling and bending the direct martensite transformation was indicated in the sample (Fig. 4). These apparent plastic deformations can be recovered completely during heating,

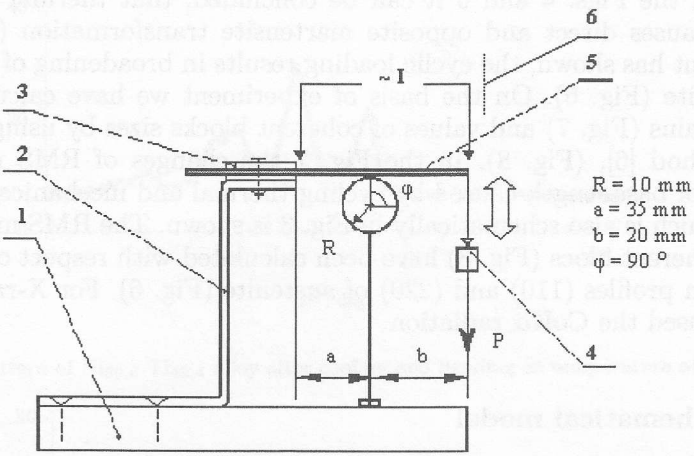


Fig. 1. Schematic diagram of the experimental setup.

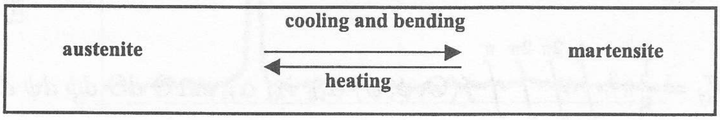


Fig. 2. Scheme of thermal and mechanical loading.

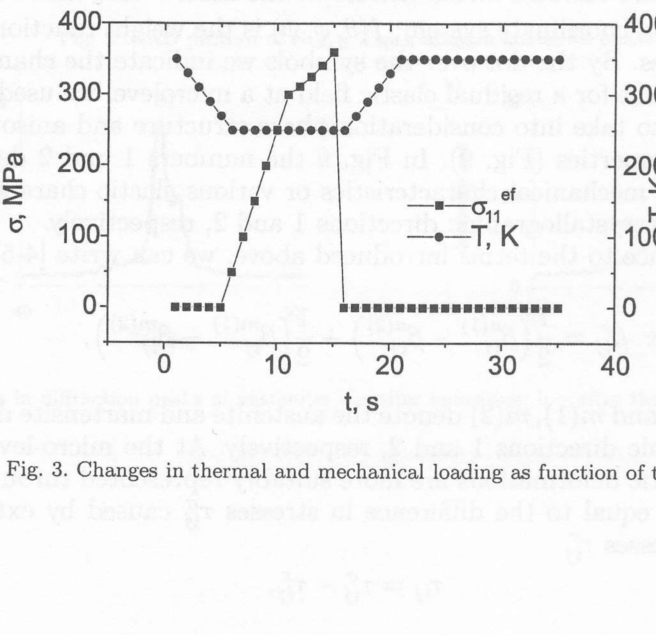


Fig. 3. Changes in thermal and mechanical loading as function of time.

resulting in the original *hot shape*, i.e., we obtain the austenite phase (Fig. 5).

From the Figs. 4 and 5 it can be concluded, that thermal and mechanical loading causes direct and opposite martensite transformation (Fig. 6). As the experiment has shown, the cyclic loading results in broadening of diffraction lines of austenite (Fig. 6). On the basis of experiment we have calculated the RMS micro-strains (Fig. 7) and values of coherent blocks sizes by using harmonic analysis method [6], (Fig. 8). In the Fig. 7 the changes of RMS micro-strains as function of base length caused by cycling thermal and mechanical loading is presented which is also schematically in Fig. 3 is shown. The RMS micro-strains and size of coherent blocs (Fig. 8) have been calculated with respect of the changes in diffraction profiles (110) and (220) of austenite (Fig. 6). For X-ray measurement we have used the CoK$\alpha$ radiation.

## 3. Mathematical model

In this section we present a mathematical model that has been used to account for physical fields during cyclic thermal and mechanical loading. The model based on the angular space averaging of the processes occurring on a micro-level can be expressed as [3]

$$\sigma_{ij}^{r} = \frac{1}{8}\pi^{2} \int_{0}^{t}\int_{0}^{2\pi}\int_{0}^{2\pi}\int_{0}^{\pi} f(\Theta,\phi,\psi)\,\alpha_{ik}\,\dot{\tau}_{kl}\,\alpha_{ji}\sin\Theta\,d\Theta\,d\phi\,d\psi\,dt, \tag{1}$$

where: $(\sigma_{ij}^{r},\theta_{kl}^{r})$ are residual stress tensors at the macro- and micro-levels; $\alpha_{jl}$ is rotation matrix of coordinate system; $f(\theta,\phi,\psi)$ is the weight function; $\theta,\phi,\psi$ are the Euler's angles. By the dot over the symbols we indicate the change of values in time. To account for a residual elastic field at a microlevel we used mechanical model allowing to take into consideration phase structure and anisotropy of the lattice elastic properties (Fig. 9). In Fig. 9 the numbers 1 and 2 denote phases with the various mechanical characteristics or various elastic characteristics of a crystal lattice in crystallographic directions 1 and 2, respectively.

With reference to the terms introduced above, we can write [4-5].

$$\beta_{ij}^{r} = \frac{1}{2}\left(\beta_{ij}^{a(1)} - \beta_{ij}^{a(2)}\right) + \frac{1}{2}\left(\beta_{ij}^{m(1)} - \beta_{ij}^{m(2)}\right), \tag{2}$$

where $a(1), a(2)$ and $m(1), m(2)$ denote the austenite and martensite deformations in crystallographic directions 1 and 2, respectively. At the micro-level, however, the residual elastic deformations are more suitably represented through the effective elastic field equal to the difference in stresses $\tau_{ij}^{\sigma}$ caused by external forces and residual stresses $\tau_{ij}^{r}$

$$\tau_{ij} = \tau_{ij}^{\sigma} - \tau_{ij}^{r}, \tag{3}$$

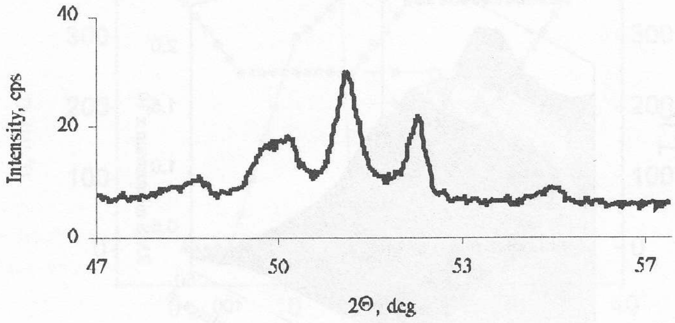


Fig. 4. XRD pattern of $Ni_{50,6}$ $Ti_{49,4}$ alloy after cooling and bending at temperature of 200 K.

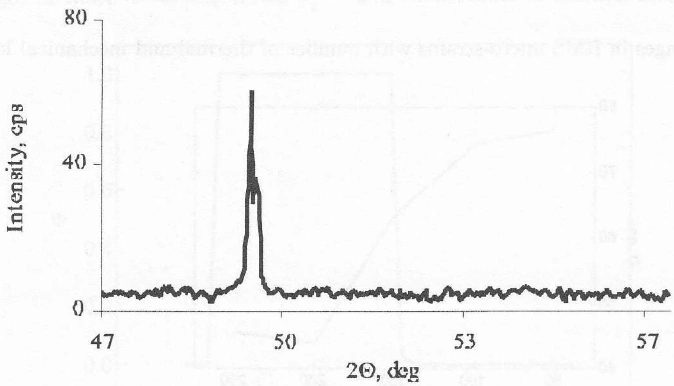


Fig. 5. XRD pattern of $Ni_{50,6}$ $Ti_{49,4}$ alloy in austenite phase.

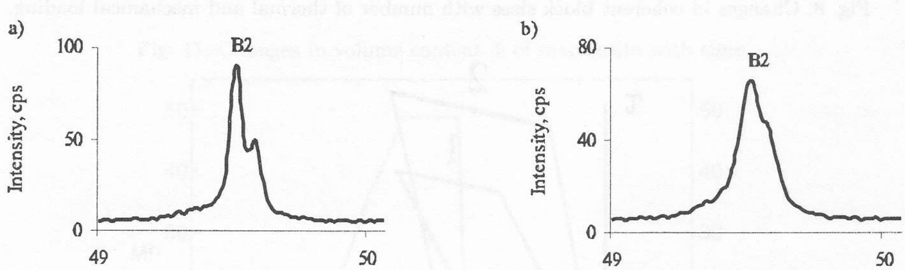


Fig. 6. Changes in diffraction peaks of austenite; a – after annealing, b – after thermal and mechanical loading.

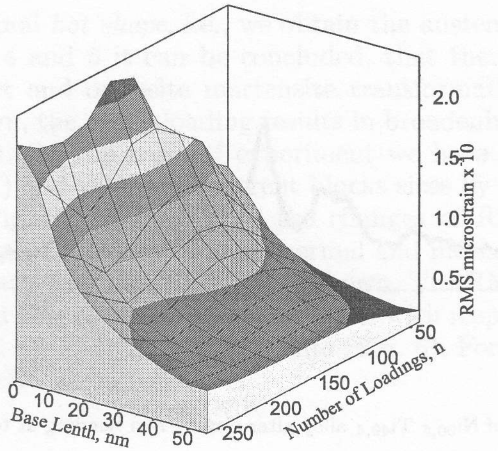


Fig. 7. Changes in RMS micro-strains with number of thermal and mechanical loading.

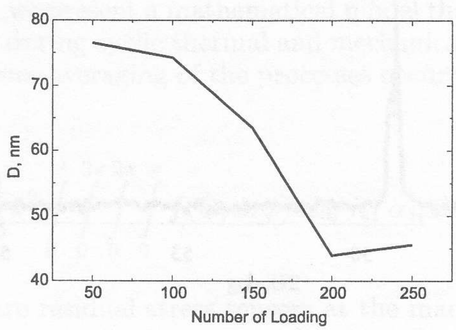


Fig. 8. Changes in coherent block sizes with number of thermal and mechanical loading.

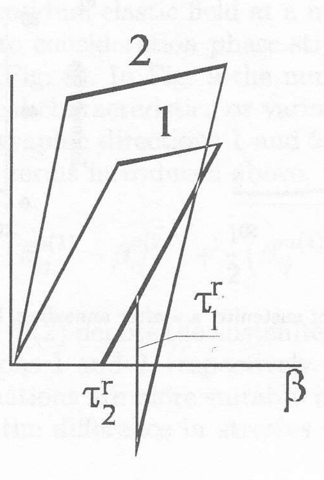


Fig. 9. Mechanical model for residual stress calculations.

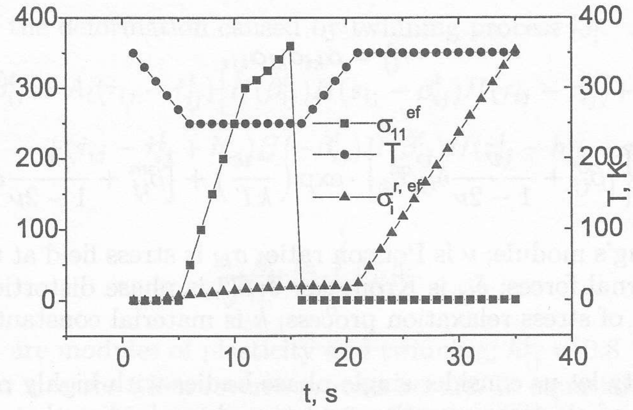


Fig. 10. Changes in effective residual stress $\sigma_i^{r,ef}$ and components of thermal and mechanical loading with time.

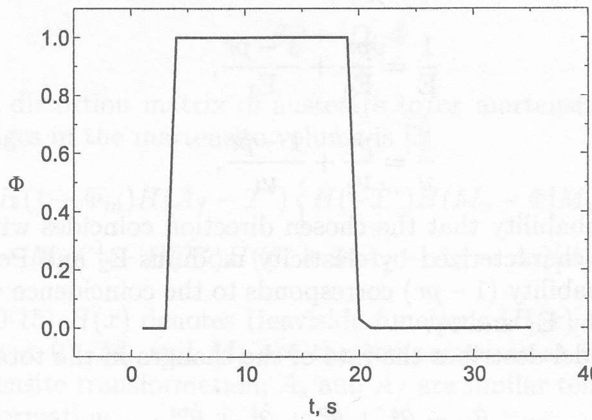


Fig. 11. Changes in volume content Φ of martensite with time.

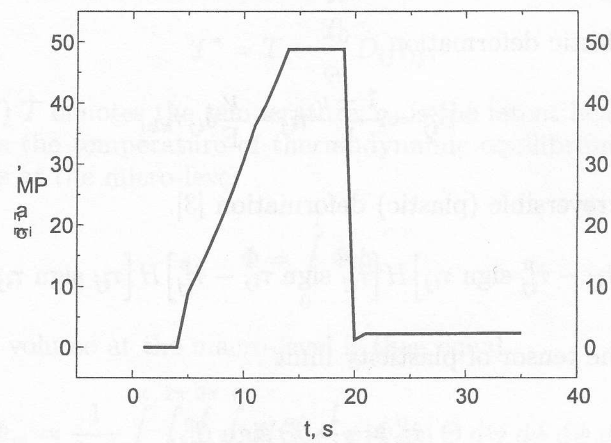


Fig. 12. Changes in intensity of residual stress in martensite $\sigma_i^{r,m}$ with time.

where

$$\tau_{ij}^{\sigma} = \alpha_{ki}\sigma_{kl}\alpha_{ij}, \tag{4}$$

and

$$\tau_{ij}^{r} = \frac{E}{1+\nu}\left\{\left[\beta_{ij}^{a} + \frac{\nu}{1-2\nu}\delta_{ij}\beta_{kk}^{a}\right]\cdot \exp\left(\frac{-w}{kT}\right) + \left[\beta_{ij}^{m} + \frac{\nu}{1-2\nu}\delta_{ij}\beta_{kk}^{m}\right]\right\}. \tag{5}$$

Here, E is Young's module; $\nu$ is Poisson ratio; $\sigma_{kl}$ is stress field at the macro-level caused by external forces; $\delta_{ij}$ is Kronecker $\delta$; $\beta_{ij}^{m}$ is phase distortion; $w$ is energy of initialization of stress relaxation process; $k$ is material constant and $T$ is temperature.

For simplicity let us consider single-phase bodies with highly represented crystal anisotropy of elastic properties, and two-phase bodies that are anisotropic at the crystallographic level. In this case the averaged modules of elasticity and Poisson ratio can be written as [4-5], [7].

$$\frac{1}{\mathrm{E}} = \frac{pr}{\mathrm{E}_2} + \frac{1-pr}{\mathrm{E}_1}, \tag{6}$$

$$\frac{1}{\nu} = \frac{pr}{\nu_2} + \frac{1-pr}{\nu_1}, \tag{7}$$

where $pr$ is the probability that the chosen direction coincides with the crystallographic direction characterized by elasticity modulus $\mathrm{E}_2$ and Poisson ratio $\nu_2$. Therefore, the probability $(1-pr)$ corresponds to the coincidence with the direction characterized by $\mathrm{E}_1$ and $\nu_1$.

The present model describes the rate of the changes in the total distortion at the micro-level

$$\dot{\beta}_{ij} = \dot{\beta}_{ij}^{e} + \dot{\beta}_{ij}^{p} + \dot{\beta}_{ij}^{t} + \dot{\beta}_{ij}^{m}. \tag{8}$$

In (8) the following abbreviations have been introduced:

- changes in elastic deformation

$$\dot{\beta}_{ij}^{e} = \frac{1+\nu}{\mathrm{E}}\dot{\tau}_{ij} - \frac{\nu}{\mathrm{E}}\delta_{ij}\dot{\tau}_{kk}, \tag{9}$$

- changes in irreversible (plastic) deformation [3].

$$\dot{\beta}_{ij}^{p} = A_p\left[\dot{\tau}_{ij} - \dot{\tau}_{ij}^{p}\ \mathrm{sign}\ \tau_{ij}\right]H\left[\tau_{ij}\ \mathrm{sign}\ \tau_{ij} - \dot{\tau}_{ij}^{p}\right]H\left[\tau_{ij}\ \mathrm{sign}\ \tau_{ij} - \dot{\tau}_{ij}^{p}\right], \tag{10}$$

- changes in the tensor of plasticity limit

$$\dot{\tau}_{ij}^{p} = \frac{1}{A_p}\dot{\beta}_{ij}^{p}\ \mathrm{sign}\ \dot{\beta}_{ij}^{p}, \tag{11}$$

- changes in the deformation caused by twinning process [3].

$$\dot{\beta}^t_{ij} = A_t(\dot{\tau}_{ij} - \dot{\tau}^t_{ij})\Big[H(\dot{\beta}^t_{ij})H(s_{ij} - \beta^t_{ij})H(\tau_{ij} - \tau^t_{ij}) + \\ +(\dot{\tau}_{ij} - \dot{\tau}^t_{ij} + h^t_{ij})H(-\dot{\beta}^t_{ij})H(\beta^t_{ij})H(\tau^t_{ij} - h^t_{ij} - \tau_{ij})\Big], \tag{12}$$

where

$$\dot{\beta}^t_{ij} = \int_0^t \dot{\beta}^t_{ij} dt, \tag{13}$$

and $A_p, A_t$ are modules of plasticity and twinning; $h^t_{ij} = 0.8\ \tau^t_{ij}$ is a change in the shear stresses when reverse process occurs. In equations (10-11) sign $x$ denotes operator of sign (sign $x = 1$ for $x > 0$ and sign $x = -1$ for $x < 0$);

- rate of the changes of the deformation caused by phase transformation

$$\dot{\beta}^m_{ij} = D_{ij}\dot{\Phi}. \tag{14}$$

Here $D_{ij}$ is the distortion matrix of austenite to/or martensite transformation; the rate of changes in the martensite volume is [3]

$$\dot{\Phi} = -\dot{T}^* H(1 - \Phi_m)H(A_f - T^*)\Big\{H(-\dot{T}^*)H(M_s - \Phi[M_s - M_f]T^*)\cdot \\ \cdot[M_s - M_f]^{-1} + H(\dot{T}^*)H(T^* + \Phi[A_f - A_s] - A_f)[A_f - A_s]^{-1}\Big\}. \tag{15}$$

In equations (10-15) $H(x)$ denotes Heaviside functions ($H(x) = 1$ for $x > 0$ and $H(x) = 0$ for $x < 0$); $M_s$ and $M_f$ are the temperatures at the beginning and end of the martensite transformation; $A_s$ and $A_f$ are similar temperatures for the austenite transformation

$$\dot{T}^* = T - \frac{T_0}{q_0} D_{ij}\dot{\tau}_{ij}, \tag{16}$$

$$T^* = T - \frac{T_0}{q_0} D_{ij}\tau_{ij}, \tag{17}$$

In equation (17) $T$ denotes the temperature; $q_0$ is the latent heat of phase transformation; $T_0$ is the temperature of thermodynamic equilibrium the martensite volume contains at the micro-level

$$\Phi = \int_0^t \dot{\Phi} dt, \tag{18}$$

The martensite volume at the macro-level is then equal

$$\Phi_m = \frac{1}{8\pi^2} \int_0^t \int_0^{2\pi} \int_0^{2\pi} \int_0^{\pi} f(\Theta, \phi, \psi)\dot{\Phi} \sin\Theta\, d\Theta\, d\phi\, d\psi\, dt, \tag{19}$$

The total deformation $\varepsilon_{ij}$ at the macro-level is

$$\varepsilon_{ij} = \frac{1}{8\pi^2}\int\limits_0^t\int\limits_0^{2\pi}\int\limits_0^{2\pi}\int\limits_0^{\pi} f(\Theta,\phi,\psi)\alpha_{ik}\dot{\beta}_{kl}\alpha_{ij}\sin\Theta\, d\Theta\, d\phi\, d\psi\, dt, \tag{20}$$

with component of total residual stresses being

$$\sigma_{ij}^{r} = \sigma_{ij}^{a} + \sigma_{ij}^{m}. \tag{21}$$

In equation (21), $\sigma_{ij}^{a}$ and $\sigma_{ij}^{m}$ designate the components of residual stress tensors in austenite and martensite, respectively. In equations (10-13) the tensor of crystallographic shift and twining $\sigma_{ij}$ is calculated as

$$\sigma_{ij} = \frac{1}{2}(\delta_{i3}\delta_{ij}\sigma_{3l} + \delta_{il}\delta_{j3}\sigma_{l3}), \tag{22}$$

and limits of shear stresses of plastic flow $\tau_{ij}^{p}$ and twinning $\tau_{ij}^{t}$ are calculated as

$$\tau_{ij}^{p} = \frac{1}{2}(\delta_{i3}\delta_{jl}\tau_{3l}^{p} + \delta_{il}\delta_{j3}\tau_{l3}^{p}), \tag{23}$$

$$\tau_{ij}^{t} = \frac{1}{2}(\delta_{i3}\delta_{jl}\tau_{3l}^{t} + \delta_{il}\delta_{j3}\tau_{l3}^{t}), \tag{24}$$

It should be noted that Heaviside functions introduced in equations (12) and (15) were developed using Boolean algebra.

## 4. Results of calculation

The mathematical model based on equations (1-24) was used to study the residual stress field evolution with the cyclic thermal and mechanical loading. The calculation of the residual stresses evolution with temperature and stress field induced by external forces were carried out with the following constants: $A_p$ = $1{\cdot}10^{-5}$ MPa$^{-1}$; $\tau_{31}^{p}$ = 200 MPa; $\nu_1$ = 0.35; $\nu_2$ = 0.3; $E_1$ = $1{\cdot}10^{5}$ MPa; $E_2$ = 0.7 $10^5$; $\tau_{31}^{t}$ = 210 MPa; $s_{31}$ = $1{\cdot}10^{-5}$; $A_t$ = $1{\cdot}10^{-5}$ MPa$^{-1}$; $T_0$ = 295 K; $q_0$ = 150 MJ$\cdot$m$^{-3}$; $M_f$ = 283 K; $M_s$ = 291 K; $A_s$ = 300 K; $A_f$ = 308 K; w = 150 kJ$\cdot$mol$^{-1}$; $k$ = 0.05. The components of martensite symmetrical transformation matrix $D_{ij}$ were determined experimentally ($D_{11}$ = – 3.013 $\cdot$ $10^{-3}$; $D_{22}$ = – 2.129 $\cdot$ $10^{-1}$; $D_{33}$ = 8.197$\cdot$ $10^{-1}$; $D_{13}$ = 4.975$\cdot$ $10^{-2}$; $D_{12}$ = 0; $D_{23}$ = 0). The results of calculation are presented in Figs. 10 to 15. The curves show the changes of structural parameters in the form of simulated loading, temperatures and time during one thermal and mechanical loading. This process is realized in less time than one minute, similarly as in the experiment. In the Fig. 10 is visible the characteristic bend at the top of $\sigma_{ij}^{ef}$ curve. It shows the influence of effective

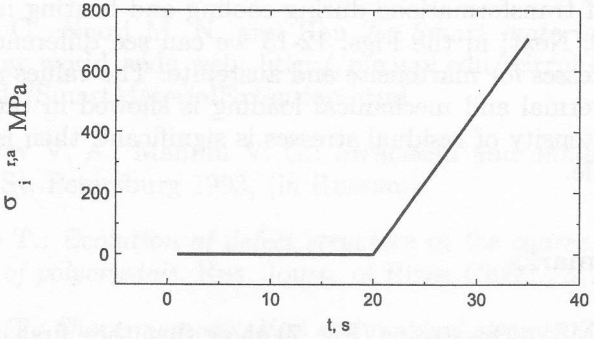


Fig. 13. Changes in intensity of residual stress in austenite $\sigma_i^{r,a}$ with time.

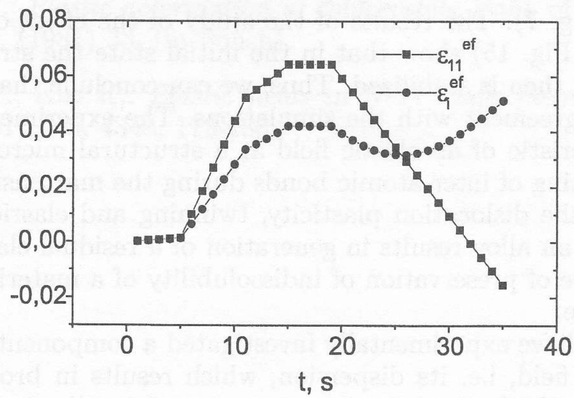


Fig. 14. Changes in component $\varepsilon_{1l}^{ef}$ and intensity $\varepsilon_i^{ef}$ of effective strains with time.

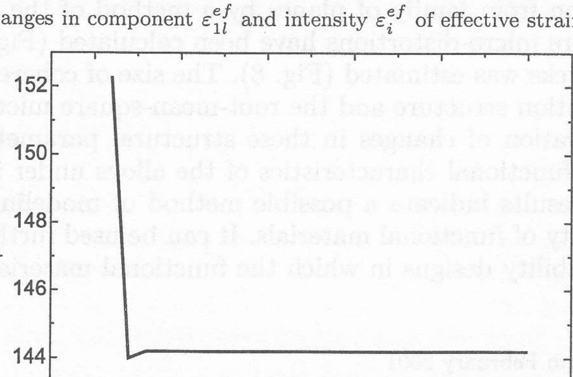


Fig. 15. Changes in intensity of residual stress: $\sigma_i^r$ with cycles of thermal and mechanical loading.

residual stresses. In the Fig. 11 are presented the changes of martensite crystal size include kinetic of transformations during cooling and heating in the sign of effective temperature. Next, in the Figs. 12-13 we can see difference in the intensity of residual stresses for martensite and austenite. The values are different. Influence of cyclic thermal and mechanical loading is showed in the Fig. 15. In the first cycles the intensity of residual stresses is significant, then is undergoing reduction and is stable.

## 5. Concluding remarks

The changes in RMS micro-strains (Fig. 7) show that they first increase with the growing number of thermal and mechanical loading cycles and then stabilize. It is clearly visible that after averaging the RMS micro-strains in base length are equal 55 nm (Fig. 7). The results of the study of the effect of the intensity of residual stresses (Fig. 15) show that in the initial state the stress intensity is sharply reduced and then is stabilized. Thus, we can conclude that experimental results show good agreement with the simulations. The experimental results represent the characteristic of an elastic field at a structural micro-level. The set of processes of breaking of inter-atomic bonds during the martensite transformation, realization of the dislocation plasticity, twinning and elastic deformations in micro-volumes of an alloy results in generation of a residual elastic field. This field is a consequence of preservation of indissolubility of a material with defects of a crystal structure.

In this paper we have experimentally investigated a component of the average action of an elastic field, i.e. its dispersion, which results in broadening of the diffraction peaks. On the basis of the measurements of distribution of intensity of two orders reflection from family of planes by a method of the harmonic analysis root-mean-square micro-distortions have been calculated (Fig. 7) and average size of coherent blocks was estimated (Fig. 8). The size of coherent blocks is connected with dislocation structure and the root-mean-square micro-distortions. In general, the observation of changes in these structural parameters allows us to estimate expected functional characteristics of the alloys under investigation.

The obtained results indicate a possible method of modeling of the serviceability and reliability of functional materials. It can be used further for numerical estimations of reliability designs in which the functional materials are applied.

Received in revised form February 2001

## References

[1] Stalmans R. and Van Humbeeck J.: *Shape memory alloys: functional and smart*; at world wide web: http://www.mtm.kuleuven/Research/Physical/

ShapeMem/smatex.htm (1996).

[2] Shakeri C., Noori M. N. and Hou Z.: *Smart materials and structures; A review*; at world wide web: http://me.wpi.edu/'cirruc/Publications/Smart-Materials/SmartMaterialExtension.html.

[3] Likhachev V. A., Malinin V. G.: *Structural and analytical strength theory*, Nauka, St. Petersburg 1993, (in Russian).

[4] Breczko T.: *Evolution of defect structure in the course of irreversible deformation of polycrystals*, Rus. Journ. of Phys. Chem., 8(1995), 1376.

[5] Breczko T.: *Shape memory effect and residual stresses*, Tech. Phys., 41(1996), 1123 (American Institute of Physics).

[6] Breczko T.: *Plastic deformation of polycrystals*, Pabl. of Bialystok Technical University, (1981) 33, (in Polish).

[7] Breczko T., Kus K.: *Elastic fields in NiTi shape memory alloys*, Proc. of SPIE (2001), vol. 4348, 173-188.